HHS Public Access

Author manuscript

Anal Chim Acta. Author manuscript; available in PMC 2020 May 16.

Published in final edited form as:

Anal Chim Acta. 2019 May 16; 1056: 88–95. doi:10.1016/j.aca.2019.01.026.

Janus Electrochemistry: Simultaneous Electrochemical Detection at Multiple Working Conditions in a Paper-based Analytical Device

Siriwan Nantaphol[a,1], **Alyssa A. Kava**[b,1], **Robert B. Channon**[b], **Takeshi Kondo**[c], **Weena Siangproh**[d], **Orawon Chailapakul**[a,*], **Charles S. Henry**[b,*]

[a]Department of Chemistry, Faculty of Science, Chulalongkorn University, Patumwan, Bangkok 10330, Thailand [b]Department of Chemistry, Colorado State University, Fort Collins, CO, 80523, United States [c]Department of Pure and Applied Chemistry, Faculty of Science and Technology, Tokyo University of Science, 2641 Yamazaki, Noda, Chiba 278–8510, Japan [d]Department of Chemistry, Faculty of Science, Srinakharinwirot University, Sukhumvit 23, Wattana, Bangkok 10110, Thailand

Abstract

The simultaneous detection of multiple analytes from a single sample is a critical tool for the analysis of real world samples. However, this is challenging to accomplish in the field by current electroanalytical techniques, where tuning assay conditions towards a target analyte often results in poor selectivity and sensitivity for other species in the mixture. In this work, an electrochemical paper-based analytical device (ePAD) capable of performing simultaneous electrochemical experiments in different solution conditions on a single sample was developed for the first time. We refer to the system as a Janus-ePAD after the two-faced Greek god because of the ability of the device to perform electrochemistry on the same sample under differing solution conditions at the same time with a single potentiostat. In a Janus-ePAD, a sample wicks down two channels from a single inlet towards two discreet reagent zones that adjust solution conditions, such as pH, before flow termination in two electrochemical detection zones. These zones feature independent working electrodes and shared reference and counter electrodes, facilitating simultaneous detection of multiple species at each species' optimal solution condition. The device utility and applicability are demonstrated through the simultaneous detection of two biologically relevant species (norepinephrine and serotonin) and a common enzymatic assay product (p-aminophenol) at two different solution pH conditions. Janus-ePADs show great promise as an inexpensive and broadly applicable platform which can reduce the complexity and/or number of steps required in

*Corresponding authors.

[1]Authors contributed equally to this work

Declaration of Interest Statement

The authors declare no conflicts of interest.

multiplexed analysis, while also operating under the optimized conditions of each species present in a mixture.

INTRODUCTION

Methods for detecting multiple analytes simultaneously at the point-of-need are of significant interest in many fields including clinical diagnostics,[1, 2] environmental monitoring,[3, 4] and food safety.[5, 6] Multiplexed analysis typically minimizes the required sample volumes, the ease and time of analysis, and/or cost of sensing. However, it is challenging to quantify multiple species - where each species requires unique conditions, from a single sample in one device using simple analyses. Frequently, target analytes are present at lower concentrations than background species[7] and matrix effects can inhibit detection.[8] Moreover, each species may require different detection settings such as detection technique, assay reagents, buffer type, and/or pH conditions, as well as intricate modifications to the sensing surface to impart selectivity. This leads to difficulties in setting experimental conditions for sensing of each analyte, often resulting in diminished sensitivity and selectivity for one or more species in the mixture, or the requirement for altogether separate detection methods or steps.[7] Integrated platforms or arrays of multiple sensors have been applied to multiplexed detection.[9–12] These sensors are usually designed with experimental conditions specific to a single target analyte, whereby separate preparation procedures are required. However, this is insufficient for point-of-care (POC) diagnostics as an individual procedures for the detection of each analyte increases the analysis time, cost, material requirements and training required for an end-user.

In 2007, Whitesides and coworkers demonstrated the first microfluidic paper-based analytical device (μPAD).[13] The device was used to perform multiplexed bioassays; since this work, μPADs have been developed extensively for use in POC settings. μPADs are an attractive platform for multiplexed POC testing as a result of their low cost, portability, low sample consumption, ease of use, and disposability.[14] Flow is generated via capillary action, precluding the need for mechanical or electrical pumps associated with traditional microfluidic devices.[15] The porous paper matrix allows for storage of dried reagents,[16] facilitating multi-step assays.[17] Through patterning with hydrophobic barriers, multiple fluidic channels can be generated on a single paper device for multiplexing.[18, 19] Colorimetric μPADs featuring multiple channels have been demonstrated extensively for multiplexed detection, where the intensity or hue of a color change corresponds to the target analyte concentration.[20–22] Despite their inherent simplicity, colorimetric μPADs are limited by the requirement for a colorimetric substrate and poor detection limits and/or sensitivity.[23–25] Additionally, splitting a sample into multiple channels results in a decrease in the total number of moles of analyte available to produce a detectable color change, negatively impacting detection limits.[26]

Electrochemical PADs (ePADs) provide a more quantitative detection method with lower detection limits, increased sensitivity, rapid measurement times (<1 min), and amenability to miniaturization.[27] Electrochemical detection is an appealing approach for multiplexed detection, as through control of the applied potential, multiple species in a mixture can be

detected in one measurement. However, this is insufficient when the target species exhibit similar redox potentials, resulting in unresolved signals. In this case, the signals can sometimes be resolved through pretreatments such as derivatization or chromatographic separations, both of which are unsuited for POC sensing. Simultaneous electrochemical sensing of multiple species without pretreatment can also be performed using chemically modified electrodes (CMEs).[28–31] CMEs and arrays of CMEs have been incorporated into ePADs for multiplexed detection of cancer biomarkers,[32, 33] heavy metals in environmental[34] and human serum samples,[35] and an array of other environmental and biological analytes. Still, the electrochemical experiments typically take place under a single set of conditions, including pH, ionic strength, and solvent. This becomes problematic for multiple-analyte detection as these parameters influence reaction rates and sensitivities and the optimal conditions are frequently analyte specific.[36–38] Solution pH is a critical variable, as pH controls metal speciation, redox potentials due to the concomitant transfer of protons or hydroxide ions, and acid-base equilibria of species whose electroactivity is a function of association or dissociation.[36–38] Often times, sensitivity is sacrificed for one or more species in a mixture by performing analysis at a single pH.[39] Methods to electrochemically control pH conditions in situ via the electrolysis of water for the detection of a single pH sensitive species have been reported.[37, 40] However, one would ideally conduct electrochemical analysis on a single aliquot, at the optimal detection conditions for each individual analyte present simultaneously.

In this work, we demonstrate a Janus-ePAD for performing multiplexed detection with the capability for in situ pH control for optimized electrochemistry. Unlike prior reports where solution conditions were static in the device, our system has the ability to generate multiple conditions in a single device from a single sample. Janus-ePADs are demonstrated for two applications; the simultaneous detection of norepinephrine (NE) and serotonin (5-hydroxytryptamine, 5-HT) and the detection of p-aminophenol (pAP). NE and 5-HT are of significant interest since their electrochemical behaviors are pH dependent[41] and low levels of NE and 5-HT are linked to several disorders, including depression, migraine, and anxiety disorders.[42] pAP is often detected as the electrochemically active product in a variety of enzymatic assays and is an important clinical and environmental contaminant.[23] Since enzyme activity is pH dependent and enzyme specific, performing multiple enzymatic assays at each enzymes' optimal pH conditions from one sample is challenging. As a proof of concept, the target analytes (NE, 5-HT and pAP) are detected at two different pH values, pH 6.0 and pH 8.0, in a single device featuring in situ pH generation. Janus-ePADs provide a new approach for the fabrication of high performance multiplexed sensing devices and has broad reaching implications for simultaneous electrochemical detection of multiple species at the POC.

EXPERIMENTAL SECTION

Chemicals, materials, and equipment

All chemicals were analytical grade and used as received, and all solutions were prepared using purified water (18.2 MΩ cm) from a Milli-Q Millipore water purification system. 5-HT was acquired from Alfa Aesar (Ward Hill, MA). NE, potassium phosphate monobasic,

sodium phosphate dibasic, phosphoric acid (H_3PO_4), sodium hydroxide (NaOH) were acquired from Sigma-Aldrich (St. Louis, MO). Potassium ferrocyanide ($Fe(CN)_6^{4-}$) was acquired from Mallinckrodt (St. Louis, MO). Graphene oxide (GO) was acquired from XF Nano, Inc. (Nanjing, China). Light mineral oil was acquired from Fischer Scientific (New Jersey). pH-indicator strips with a pH range of 4.0 – 7.0 and 6.5 – 10.0 were acquired from Merck (Darmstadt, Germany). Whatman 4 chromatography paper was acquired from Fisher Scientific (Pittsburgh, PA). A XEROX Phaser 8860 printer was used to print wax patterns on PADs following established protocols. An Isotemp hot plate from Fischer Scientific, set at 150°C, was used to melt the wax on the paper. Ag/AgCl ink from Gwent Group (Torfaen, U.K.) was used to construct the conducting pads and reference electrode (RE). Carbon ink from Ercon Incorporated (Wareham, MA) was used for the construction of the counter electrode (CE). Boron doped diamond (BDD) powder was prepared through a previously reported procedure.[43] The fabrication of the working electrode (WE) of BDD paste electrode (BDDPE) followed the procedure described previously.[44] Stencil-printed Ag/AgCl on a transparency sheet substrate was prepared as a conducting pad. To minimize BDD paste consumption, an electrode body containing three smaller openings (0.1 × 2 mm rectangles) was fabricated using a laser engraving system (Epilog, Golden, CO). The BDDPE was prepared by mixing BDD powder and mineral oil (70:30, w/w) and filled into the electrode body.

Device fabrication and operation

The design, details of the fabrication procedures and operation of the Janus-ePAD is shown in Figure 1. Adobe Illustrator CS6 software was used to design device features containing sample reservoir, two reagent zones and two detection zones. After printing the design using a wax printer (Xerox Colorqube 8870), devices were heated on a hot plate at 175 °C for 50 s to melt the wax through the paper, creating a hydrophobic barrier. The backs of the paper devices, except the detection zones, were taped with Scotch packing tape to control fluid flow and prevent leaking during the measurements. The electrochemical detection zone consists of three layers: (i) CE and RE fabricated on 8 mm diameter circular hydrophilic areas at the back side of wax-printed paper by stencil-printing, (ii) Whatman #4 paper pieces inserted between the stencil-printed electrodes paper layer and WE layer to improve the efficiency for the solution flow in the channel, and (iii) the BDDPEs. Two different pH values of pH 6.0 and 8.0 can be generated by adding three 1.4 μL aliquots of 0.5 M H_3PO_4 to the 1st reagent zone and three 1.4 μL aliquots of 0.5 M NaOH to the 2nd reagent zone. All reagents and samples were applied on the front (wax-printed) side of device. Between each reagent addition, the device was dried at room temperature.

For the measurement step, a polydimethylsiloxane (PDMS) lid was placed on the top of device for applying equal pressure across the paper surface, thus controlling the flow rates. A 60 μL aliquot of sample solution was gently introduced into the device at the sample reservoir through the hole in the PDMS lid, capillary action carried solution along the channels (the wax barrier served to confine and direct sample flow). As the solution reacted with the H_3PO_4 and NaOH deposited at the reagent zones, pH values of solution were adjusted to pH 6.0 and 8.0, respectively. After the adjusted pH solutions flowed to detection zones, the PDMS lid was removed and electrochemical detection was performed.

Electrochemical Detection

All electrochemical experiments were performed using a model CHI832 bipotentiostat (CH Instruments, Austin, TX) with four-electrode configuration including a reference electrode (RE), a counter electrode (CE), and two working electrodes (WEs). All measurements were carried out at room temperature (22±1°C). For NE and 5-HT detection, an electrochemically reduced graphene oxide-modified BDDPE (ERGO-BDDPE) was used as the WE for NE and 5-HT detection in an attempt to enable simultaneous detection of both compounds as described in our previous work.[44] Details of the ERGO-modified electrode preparation are described in Supporting Information, section 1. Standard solutions of NE and 5-HT were prepared in 0.1 M phosphate buffer (PB) pH 7.0, and a 60 μL aliquot was used for the experiments. Differential pulse voltammetry (DPV) was employed for NE and 5-HT detection with an amplitude of 60 mV, potential increment of 4 Hz, and a pulse width of 0.05 s. Electrochemical detection of p-aminophenol (pAP, EMD Milipore, Billerica, MA) was carried out using differential pulse voltammetry (DPV). For DPV, a pulse amplitude of 50 mV, potential increment of 4 Hz, and a pulse width of 0.1 s were used.

RESULTS AND DISCUSSION

Electrochemical characterization of the Janus-ePAD

To validate the Janus-ePAD, $Fe(CN)_6^{4-}$ cyclic voltammetry was investigated with the two detection zones / working electrodes. As shown in Figure 2, the BDDPEs exhibit well-defined and symmetrical anodic and cathodic peaks, with similar peak currents and peak potentials between the two working electrodes (4.23 ± 0.03 (i_{pa1}) vs 4.55 ± 0.18 (i_{pa2}) μA, −4.22 ± 0.11 (i_{pc1}) vs −4.61 ± 0.09 (i_{pc2}) μA, 0.21 ± 0.01 (E_{pa1}) vs 0.23 ± 0.01 (E_{pa2}) V, and −0.10 ± 0.02 (E_{pc1}) vs −0.12 ± 0.02 (E_{pc2}) V vs Ag/AgCl). The average peak potential separation (ΔE_p) was found to be 311 ± 12, and 351 ± 13 mV for BDDPE1 and BDDPE2, respectively ($n = 3$). Due to its inner sphere electrocatalytic nature, $Fe(CN)_6^{4-}$ exhibits electrochemical irreversibility at the BDDPEs. The electron transfer kinetics of this species are impeded at oxygen terminated BDD and large ΔE_p values have been frequently observed at oxygen terminated BDD.[45, 46]

In situ pH adjustment in a Janus-ePAD

To carry out on-line adjustment of phosphate buffer pH from pH 7.0 to pH 6.0 or 8.0, 0.5 M H_3PO_4 and 0.5 M NaOH were dried on the two reagent zones and pH-indicator strips were used to measure the solution pH in the detection zone. The parameters influencing the adjustment of pH values were optimized including volume of sample/standard solution and volume of H_3PO_4 and NaOH solution.

The sample volume needed to wet the channels, reagent zones, and detection zones, was initially investigated. Three 1.0 μL aliquots each of 0.50 M H_3PO_4 and 0.50 M NaOH solutions were added into 1st reagent zone and 2nd reagent zone, respectively. Next, 45 to 65 μL of 0.10 M PB pH 7.0 solution was added into the sample zone. The pH-indicator strips were placed on the bottom of each detection zones to observe the pH change and the solution homogeneity after pH adjustment. The results are shown in Figure 3(a). Homogeneous color change on pH-indicator strips, indicating full wetting, was observed at

65 μL, and consequently, 65 μL was chosen as the optimum condition. The amount of H_3PO_4 and NaOH is another important factor in the adjustment of pH value. Therefore, 0.50 μL to 1.8 μL of 0.50 M H_3PO_4 and 0.50 M NaOH was added to the 1st 3 4 reagent zone and the 2nd reagent zone, respectively, and 65 μL of 0.10 M PB pH 7.0 was applied to the sample reservoir of the device to determine the optimal volume for adjusting pH on each side of detection zones to pH 6.0 and pH 8.0. The pH-indicator strip was used to observe the change in solution pH reaching the detection zones. As shown in Figure 3(b), the optimal volume of 0.50 M H_3PO_4 and 0.50 M NaOH that can adjust the solution pH from pH 7.0 to pH 6.0 or pH 8.0 was 1.4 μL.

Neurotransmitter detection

NE and 5-HT are important catecholamine neurotransmitters in biological samples. The simultaneous detection of these compounds is of great importance since low levels of NE and 5-HT have been correlated to several disorders, including depression, migraines, and anxiety.[42] NE and 5-HT have similar oxidation potentials and cannot be discriminated using bare BDDPEs.[44] In contrast, electrochemically reduced graphene oxide modified BDDPEs (ERGO-BDDPE) can differentiate peak potentials, enabling simultaneous analyte detection.[44] Figure 4(a) shows the DPVs of NE and 5-HT at ERGO-BDDPE at different pH conditions. The redox behavior of NE and 5-HT are pH dependent, with shifting overpotentials and peak currents as a function of pH. Clearly NE and 5-HT show preference for differing pH conditions, with maximum oxidation currents for NE and 5-HT at pH 6.0 and pH 8.0 respectively as shown in Figure 4(b).

Electrochemical behavior of NE and 5-HT on Janus-ePAD

Differential pulse voltammetry (DPV) was used to evaluate the performance of the Janus-ePAD for simultaneous detection of NE and 5-HT under their respective optimal pH conditions. Initially, a solution consisting of 25 μM NE and 10 μM 5-HT was prepared in 0.10 M PB pH 7.0. The solution pH can be simultaneously adjusted to pH 6.0, and pH 8.0 by impregnating the reagent zones with H_3PO_4 and NaOH respectively. DPVs of NE and 5-HT at the ERGO-BDDPE1 and ERGO-BDDPE2 are shown in Figure 5. At the ERGO-BDDPE1 (pH 6.0), NE and 5-HT exhibit oxidative peaks at 0.02 ± 0.01 and 0.15 ± 0.04 V vs. Ag/AgCl respectively, with peak oxidation currents of NE and 5-HT was 0.40 ± 0.02 and 0.12 ± 0.04 μA respectively. For the ERGO-BDDE2 (pH 8.0), the oxidation peak of NE and 5-HT occurs at potential of −0.053 ± 0.042 and 0.10 ± 0.02 V vs. Ag/AgCl, respectively, and the oxidation current of NE and 5-HT was 0.31 ± 0.05 and 0.25 ± 0.04 μA, respectively. From these results, it can be observed that at ERGO-BDDPE2 (pH 8.0), the oxidation peak potential of NE and 5-HT occurs at more negative values compared to ERGO-BDDPE1 (pH 6.0). The highest peak current of NE was observed at ERGO-BDDPE1 (pH 6.0) while the highest peak current of 5-HT was observed at ERGO-BDDPE2 (pH 8.0). These results were in accordance with the results shown Figure 4, indicating that the Janus-ePAD can be used to simultaneously detect NE and 5-HT at each species' optimized pH conditions.

Janus-ePAD Detection Zone Design

The design of the Janus-ePAD also influences the performance. Three different designs were fabricated as shown in Figure S2(a). For the 1st design, the CE and RE were fabricated on

the wax-patterned paper and the WE sections were attached on the wax-patterned device side opposite to the screen-printed CE and RE. For the 2nd design, the WEs were attached to the device on the screen-printed CE and RE side. For the 3rd design, the CE and RE section were fabricated on a separate piece of wax-printed paper which was attached on the top of wax-patterned paper and the WE sections were attached on the bottom of the device. Figure S2(b) and S2(c) show the comparison of peak currents of NE and 5-HT at pH 6.0 and 8.0 obtained from different designs of Janus-ePAD. The oxidation peak current of NE and 5-HT for the 2nd design is the highest. This is due to the smallest distance between electrodes and paper and all electrodes being completely covered by sample solution in the 2nd platform. In case of the 1st and 3rd platforms, the low sensitivity may be a result of poor sample solution coverage of the electrodes. The surfaces of the BDD electrodes are hydrophobic as a result of the mineral oil binder, while the commercial inks used render the CE and RE hydrophobic as well. The hydrophobicity of these surfaces likely leads to poor wetting of the electrode surface at the end of the paper channels. The porous cellulose matrix of the paper channel may also not be 100% saturated as fluid saturation decreases as the fluid front distance increases from the source.[47]

Analytical performance

Using the optimized conditions, the analytical performance of the device for NE and 5-HT detection was evaluated. As shown in Figure 6, the peak currents of NE or 5-HT increased linearly with increasing concentration. For NE detection, at the ERGO-BDDPE1 (pH 6.0), a linear calibration plot was found over a range of 5.0 – 75 μM with a sensitivity of 0.019 μA μM^{-1} and correlation coefficient (R^2) of 0.9849. At the ERGO-BDDPE2 (pH 8.0), a linear calibration plot was found over a range of 10 – 75 μM with a sensitivity of 0.012 μA μM^{-1} and correlation coefficient (R^2) of 0.9890. For 5-HT, at the ERGO-BDDPE1 (pH 6.0), a linear calibration plot was obtained over a range of 1.0 – 10 μM with a sensitivity of 0.017 μA μM^{-1} and R^2 of 0.9928. For the ERGO-BDDPE2, a linear calibration plot was obtained over a range of 0.5–10 μM with a sensitivity of 0.027 μA μM^{-1} and R^2 of 0.9909. The LODs (3SDblank/slope) were 0.71 and 0.54 μM for NE and 5-HT, respectively, for the ERGO-BDDPE1 (pH 6.0). The LODs of NE and 5-HT were 1.2, and 0.38 μM, respectively, for the ERGO-BDDPE2 (pH 8.0). The analytical performance of these two electrodes is summarized in Table S1.

pAP detection

Enzymatic assays are important detection motifs as a result of an enzymes inherent selectivity toward target analytes.[48] Important applications of enzymatic assays include clinical diagnostics, in enzyme linked immunosorbent assays (ELISAs), and in bacteria detection, where enzymes produced by bacteria can be monitored in order to detect and identify bacteria.[23, 48, 49] For example, β-Galactosidase (β-Gal) activity is often monitored to detect *E. coli* contamination via the production of the electrochemically active molecule p-aminophenol (pAP) from p-aminophenylgalactopyranoside (pAPG) substrate hydrolysis.[23] Here, we demonstrate the simultaneous detection of pAP at two pH conditions in the Janus-ePAD as both the enzymatic activity and the electrochemical detection of the product are pH dependent processes. Multiplexed enzymatic assays have been demonstrated on ePADs, for example, Dungchai et al. simultaneously determined uric

acid, lactate, and glucose, however, each system was analyzed separately.[50] It would be ideal to perform the assays at each enzymes' optimal solution pH thus improving both sensitivity and detection limits. This proof of concept is demonstrated as we believe the Janus-ePAD would ultimately be used to perform multiplexed enzymatic assays at each enzymes' optimal pH conditions, and as such, pAP serves as a model analyte for these applications.

The optimized conditions for on line pH generation as discussed above were used and pAP was detected at BDDPE1 (pH 8.0) and BDDPE2 (pH 6.0). As shown in Figure 7, upon in situ pH generation, the peak potential and height for pAP oxidation vary with pH (Figure 7b) as compared to the response obtained at BDDPE1 and BDDPE2 when both cells operate at pH 7.0 (Figure 7a). As the pH increases, the overpotential required to oxidize pAP decreases. As demonstrated in the calibration curves for pAP obtained under dual pH conditions in the Janus-ePAD (Figure 7c), the sensitivity increases by about a factor of 2, increasing the pH from pH 6.0 (0.0022 μA μM^{-1}) to pH 8.0 (0.0040 μA μM^{-1}). Of note here is the larger standard deviations obtained at unmodified BDDPEs, which range from 15% to 47% of the average peak current (n = 3 devices). Upon further studies, it was found that the presence of the mineral oil pasting liquid at the surface of the BDDPE contributes to two phenomena that impact the reproducibility of the electrode response in the ePAD: i) time-dependent extraction and subsequent pre-concentration of organic analytes (e.g. pAP) and ii) slow electron transfer kinetics due the inhibitive layers of pasting liquid at the electrode surface. Both of these phenomena are commonly observed with carbon paste electrodes, however, when the electrodes are utilized in bulk solutions, dissolution of these inhibitory pasting liquid molecules occurs immediately upon immersion in solution, and the electrode surface is sufficiently active, while still being prone to analyte extraction.[51, 52] It was found in this work, that in the paper-based device, this dissolution and subsequent activation is a slow, time-dependent process as a result of small volumes confined to the cellulose matrix at the electrode surface. For this reason, further studies are being carried out to activate the BDDPEs prior to device fabrication so as to eliminate this time-dependent and variable activation process. This, we believe, is the reason the pre-modified ERGO-BDDPEs provide more reproducible results, as the electrode surface is modified and thus activated prior to attachment and use in the Janus-ePAD. Despite the poor reproducibility obtained as a result of the unmodified BDDPEs, this work, to the best of our knowledge, is the first demonstration of applying multiple solution chemistries to a single sample simultaneously in a paper-based device.

CONCLUSION

A Janus electrochemical paper-based analytical device (Janus-ePAD) was described for the first time. This device exploits the ability to pattern paper with multiple fluidic channels and store dried reagents in specific zones to perform solution condition adjustment and electrochemical detection in multiple sets of solution conditions on single sample simultaneously. This Janus-ePAD has a wide range of implications in point-of-need paper-based diagnostics where sensitive and selective multiplexed detection is necessary, as is often the case in biomedical diagnostics, environmental monitoring, and food quality analysis.[53–55] While multiplexed colorimetric and electrochemical PADs have been

demonstrated extensively in the literature for a wide range of analytes, the reported ePADs have not yet addressed the sensitivity of redox reactions to solution chemistry, and have largely relied upon highly analyte specific chemically modified electrode (CME) systems.[7, 56] To offer a solution to this problem, in this work, the solution pH was adjusted on line to carry out electrochemical detection of serotonin and norepinephrine at each species' optimal solution pH. p-aminophenol was also detected in two pH conditions simultaneously as a proof-of-concept towards multiplexed enzymatic assays in the Janus-ePADs. In future applications, it is important to note that not only can solution conditions (ionic strength, buffer, reagents, etc) can be tuned in situ, but each detection zone may also contain either a different working electrode material or working electrodes chemically modified for optimal detection of one analyte in a mixture as well. We expect that the Janus-ePAD can be adopted for sensitive and selective multiplexed detection where analytes require different experimental conditions such as buffer type, ionic strength, and/or solvent. This ePAD can reduce the complexity and/or time of analysis which an end user must carry out while maintaining the highest degree of selectivity and specificity for each species in a mixture.

Supplementary Material

Refer to Web version on PubMed Central for supplementary material.

Acknowledgements

This work was financially supported by the Thailand Research Fund via the Research Team Promotion Grant (RTA6080002). SN is grateful to the Ratchadaphiseksomphot Endowment Fund, Chulalongkorn University, for a Postdoctoral Fellowship. Funding for AK, RC, and CH was provided through a grant from the National Institutes of Health (ES024719) and the US Department of Agriculture (AP17WSNWRC00C027).

References

[1]. Pregibon DC, Toner M, Doyle PS, Multifunctional Encoded Particles for High-Throughput Biomolecule Analysis, Science, 315 (2007) 1393. [PubMed: 17347435]

[2]. Kingsmore SF, Multiplexed protein measurement: technologies and applications of protein and antibody arrays, Nature Reviews Drug Discovery, 5 (2006) 310. [PubMed: 16582876]

[3]. Mentele MM, Cunningham J, Koehler K, Volckens J, Henry CS, Microfluidic Paper-Based Analytical Device for Particulate Metals, Anal. Chem, 84 (2012) 4474–4480. [PubMed: 22489881]

[4]. Kulagina NV, Lassman ME, Ligler FS, Taitt CR, Antimicrobial Peptides for Detection of Bacteria in Biosensor Assays, Anal. Chem, 77 (2005) 6504–6508. [PubMed: 16194120]

[5]. Adkins JA, Boehle K, Friend C, Chamberlain B, Bisha B, Henry CS, Colorimetric and Electrochemical Bacteria Detection Using Printed Paper- and Transparency-Based Analytic Devices, Anal. Chem, 89 (2017) 3613–3621. [PubMed: 28225595]

[6]. Jokerst JC, Adkins JA, Bisha B, Mentele MM, Goodridge LD, Henry CS, Development of a Paper-Based Analytical Device for Colorimetric Detection of Select Foodborne Pathogens, Analytical Chemistry, 84 (2012) 2900–2907. [PubMed: 22320200]

[7]. Tanner EE, Compton RG, How can electrode surface modification benefit electroanalysis?, Electroanal., (2018).

[8]. Rodthongkum N, Ruecha N, Rangkupan R, Vachet RW, Chailapakul O, Graphene-loaded nanofiber-modified electrodes for the ultrasensitive determination of dopamine, Anal. Chim. Acta, 804 (2013) 84–91. [PubMed: 24267067]

[9]. Washburn AL, Luchansky MS, Bowman AL, Bailey RC, Quantitative, Label-Free Detection of Five Protein Biomarkers Using Multiplexed Arrays of Silicon Photonic Microring Resonators, Anal. Chem, 82 (2010) 69–72. [PubMed: 20000326]

[10]. Chen Z-P, Zhong L-J, Nordon A, Littlejohn D, Holden M, Fazenda M, Harvey L, McNeil B, Faulkner J, Morris J, Calibration of Multiplexed Fiber-Optic Spectroscopy, Anal. Chem, 83 (2011) 2655–2659. [PubMed: 21381638]

[11]. Rebe Raz S, Haasnoot W, Multiplex bioanalytical methods for food and environmental monitoring, TrAC, Trends Anal. Chem, 30 (2011) 1526–1537.

[12]. Kloth K, Niessner R, Seidel M, Development of an open stand-alone platform for regenerable automated microarrays, Biosens. Bioelectron, 24 (2009) 2106–2112. [PubMed: 19110413]

[13]. Martinez AW, Phillips ST, Butte MJ, Whitesides GM, Patterned paper as a platform for inexpensive, low-volume, portable bioassays, Angew. Chem., Int. Ed, 46 (2007) 1318–1320.

[14]. Martinez AW, Phillips ST, Whitesides GM, Carrilho E, Diagnostics for the developing world: microfluidic paper-based analytical devices, ACS Publications, 2009.

[15]. Gong MM, Sinton D, Turning the page: advancing paper-based microfluidics for broad diagnostic application, Chemical reviews, 117 (2017) 8447–8480. [PubMed: 28627178]

[16]. Rahbar M, Nesterenko PN, Paull B, Macka M, Geometrical Alignment of Multiple Fabrication Steps for Rapid Prototyping of Microfluidic Paper-Based Analytical Devices, Anal. Chem, 89 (2017) 11918–11923. [PubMed: 29090570]

[17]. Fu E, Downs C, Progress in the development and integration of fluid flow control tools in paper microfluidics, Lab on a Chip, 17 (2017) 614–628. [PubMed: 28119982]

[18]. Cate DM, Adkins JA, Mettakoonpitak J, Henry CS, Recent Developments in Paper-Based Microfluidic Devices, Analytical Chemistry, 87 (2015) 19–41. [PubMed: 25375292]

[19]. Yang Y, Noviana E, Nguyen MP, Geiss BJ, Dandy DS, Henry CS, Paper-Based Microfluidic Devices: Emerging Themes and Applications, Analytical Chemistry, 89 (2017) 71–91. [PubMed: 27936612]

[20]. Sriram G, Bhat MP, Patil P, Uthappa UT, Jung H-Y, Altalhi T, Kumeria T, Aminabhavi TM, Pai RK, Madhuprasad, Kurkuri MD, Paper-based microfluidic analytical devices for colorimetric detection of toxic ions: A review, TrAC, Trends Anal. Chem, 93 (2017) 212–227.

[21]. Creran B, Li X, Duncan B, Kim CS, Moyano DF, Rotello VM, Detection of Bacteria Using Inkjet-Printed Enzymatic Test Strips, ACS Appl. Mater. Interfaces, 6 (2014) 19525–19530. [PubMed: 25318086]

[22]. Wei X, Tian T, Jia S, Zhu Z, Ma Y, Sun J, Lin Z, Yang CJ, Microfluidic Distance Readout Sweet Hydrogel Integrated Paper-Based Analytical Device (μDiSH-PAD) for Visual Quantitative Point-of-Care Testing, Anal. Chem, 88 (2016) 2345–2352. [PubMed: 26765320]

[23]. Adkins JA, Noviana E, Henry CS, Development of a Quasi-Steady Flow Electrochemical Paper-Based Analytical Device, Analytical chemistry, 88 (2016) 10639–10647. [PubMed: 27749031]

[24]. Hossain SMZ, Brennan JD, β-Galactosidase-Based Colorimetric Paper Sensor for Determination of Heavy Metals, Anal. Chem, 83 (2011) 8772–8778. [PubMed: 22029903]

[25]. Rattanarat P, Dungchai W, Cate D, Volckens J, Chailapakul O, Henry CS, Multilayer paper-based device for colorimetric and electrochemical quantification of metals, Analytical chemistry, 86 (2014) 3555–3562. [PubMed: 24576180]

[26]. Nguyen MP, Meredith NA, Kelly SP, Henry CS, Design considerations for reducing sample loss in microfluidic paper-based analytical devices, Anal. Chim. Acta, 1017 (2018) 20–25. [PubMed: 29534791]

[27]. Nie Z, Deiss F, Liu X, Akbulut O, Whitesides GM, Integration of paper-based microfluidic devices with commercial electrochemical readers, Lab Chip, 10 (2010) 3163–3169. [PubMed: 20927458]

[28]. Fernandes SC, Walz JA, Wilson DJ, Brooks JC, Mace CR, Beyond wicking: Expanding the role of patterned paper as the foundation for an analytical platform, ACS Publications, 2017.

[29]. Gao W, Nyein HYY, Shahpar Z, Fahad HM, Chen K, Emaminejad S, Gao Y, Tai L-C, Ota H, Wu E, Bullock J, Zeng Y, Lien D-H, Javey A, Wearable Microsensor Array for Multiplexed Heavy Metal Monitoring of Body Fluids, ACS Sens., 1 (2016) 866–874.

[30]. Radha Shanmugam N, Muthukumar S, Chaudhry S, Anguiano J, Prasad S, Ultrasensitive nanostructure sensor arrays on flexible substrates for multiplexed and simultaneous electrochemical detection of a panel of cardiac biomarkers, Biosens. Bioelectron, 89 (2017) 764–772. [PubMed: 27818043]

[31]. Jampasa S, Siangproh W, Laocharoensuk R, Yanatatsaneejit P, Vilaivan T, Chailapakul O, A new DNA sensor design for the simultaneous detection of HPV type 16 and 18 DNA, Sens. Actuators, B, 265 (2018) 514–521.

[32]. Li L, Li W, Yang H, Ma C, Yu J, Yan M, Song X, Sensitive origami dual-analyte electrochemical immunodevice based on polyaniline/Au-paper electrode and multi-labeled 3D graphene sheets, Electrochim Acta, 120 (2014) 102–109.

[33]. Zang D, Ge L, Yan M, Song X, Yu J, Electrochemical immunoassay on a 3D microfluidic paper-based device, Chem. Commun, 48 (2012) 4683–4685.

[34]. Mettakoonpitak J, Mehaffy J, Volckens J, Henry CS, AgNP/Bi/Nafion-modified Disposable Electrodes for Sensitive Zn (II), Cd (II), and Pb (II) Detection in Aerosol Samples, Electroanal., 29 (2017) 880–889.

[35]. Ruecha N, Rodthongkum N, Cate DM, Volckens J, Chailapakul O, Henry CS, Sensitive electrochemical sensor using a graphene–polyaniline nanocomposite for simultaneous detection of Zn (II), Cd (II), and Pb (II), Anal. Chim. Acta, 874 (2015) 40–48. [PubMed: 25910444]

[36]. Read TL, Bitziou E, Joseph MB, Macpherson JV, In situ control of local pH using a boron doped diamond ring disk electrode: optimizing heavy metal (mercury) detection, Anal. Chem, 86 (2013) 367–371. [PubMed: 24321045]

[37]. Read TL, Joseph MB, Macpherson JV, Manipulation and measurement of pH sensitive metal–ligand binding using electrochemical proton generation and metal detection, Chem. Commun, 52 (2016) 1863–1866.

[38]. Blaho JK, Goldsby KA, Redox regulation based on the pH-dependent hydrolysis of 2-pyridinecarboxaldehyde coordinated to ruthenium (II), J. Am. Chem. Soc, 112 (1990) 6132–6133.

[39]. Chen X, Zhang G, Shi L, Pan S, Liu W, Pan H, Au/ZnO hybrid nanocatalysts impregnated in N-doped graphene for simultaneous determination of ascorbic acid, acetaminophen and dopamine, Materials Science and Engineering: C, 65 (2016) 80–89. [PubMed: 27157730]

[40]. Rassaei L, Marken F, Pulse-voltammetric glucose detection at gold junction electrodes, Anal. Chem, 82 (2010) 7063–7067. [PubMed: 20687584]

[41]. Wang Y, Wang S, Tao L, Min Q, Xiang J, Wang Q, Xie J, Yue Y, Wu S, Li X, Ding H, A disposable electrochemical sensor for simultaneous determination of norepinephrine and serotonin in rat cerebrospinal fluid based on MWNTs-ZnO/chitosan composites modified screen-printed electrode, Biosens. Bioelectron, 65 (2015) 31–38. [PubMed: 25461135]

[42]. Graeff FG, Guimaraes FS, De Andrade TG, Deakin JF, Role of 5-HT in stress, anxiety, and depression, Pharmacology, biochemistry, and behavior, 54 (1996) 129–141.

[43]. Kondo T, Sakamoto H, Kato T, Horitani M, Shitanda I, Itagaki M, Yuasa M, Screen-printed diamond electrode: A disposable sensitive electrochemical electrode, Electrochemistry Communications, 13 (2011) 1546–1549.

[44]. Nantaphol S, Channon RB, Kondo T, Siangproh W, Chailapakul O, Henry CS, Boron Doped Diamond Paste Electrodes for Microfluidic Paper-Based Analytical Devices, Anal. Chem, 89 (2017) 4100–4107. [PubMed: 28263062]

[45]. Hutton LA, Iacobini JG, Bitziou E, Channon RB, Newton ME, Macpherson JV, Examination of the factors affecting the electrochemical performance of oxygen-terminated polycrystalline boron-doped diamond electrodes, Analytical chemistry, 85 (2013) 7230–7240. [PubMed: 23790001]

[46]. Granger MC, Swain GM, The influence of surface interactions on the reversibility of Ferri/Ferrocyanide at boron-doped diamond thin-film electrodes, J Electrochem Soc, 146 (1999) 4551–4558.

[47]. Houghtaling J, Liang T, Thiessen G, Fu E, Dissolvable Bridges for Manipulating Fluid Volumes in Paper Networks, Anal. Chem, 85 (2013) 11201–11204. [PubMed: 24228812]

[48]. Adkins JA, Boehle K, Friend C, Chamberlain B, Bisha B, Henry CS, Colorimetric and electrochemical bacteria detection using printed paper-and transparency-based analytic devices, Analytical chemistry, 89 (2017) 3613–3621. [PubMed: 28225595]

[49]. Hemalatha T, UmaMaheswari T, Krithiga G, Sankaranarayanan P, Puvanakrishnan R, Enzymes in clinical medicine: an overview, Indian J. Exp. Biol, 51 (2013) 777–788. [PubMed: 24266101]

[50]. Dungchai W, Chailapakul O, Henry CS, Electrochemical Detection for Paper-Based Microfluidics, Analytical Chemistry, 81 (2009) 5821–5826. [PubMed: 19485415]

[51]. Rice ME, Galus Z, Adams RN, Graphite paste electrodes: Effects of paste composition and surface states on electron-transfer rates, J. Electroanal. Chem. Interfacial Electrochem., 143 (1983) 89–102.

[52]. Ravichandran K, Baldwin RP, Enhanced voltammetric response by electrochemical pretreatment of carbon paste electrodes, Anal. Chem, 56 (1984) 1744–1747.

[53]. Wu MY-C, Hsu M-Y, Chen S-J, Hwang D-K, Yen T-H, Cheng C-M, Point-of-care detection devices for food safety monitoring: Proactive disease prevention, Trends in biotechnology, 35 (2017) 288–300. [PubMed: 28089198]

[54]. Hu J, Wang S, Wang L, Li F, Pingguan-Murphy B, Lu TJ, Xu F, Advances in paper-based point-of-care diagnostics, Biosens. Bioelectron, 54 (2014) 585–597. [PubMed: 24333570]

[55]. Meredith NA, Quinn C, Cate DM, Reilly TH, Volckens J, Henry CS, based analytical devices for environmental analysis, Analyst, 141 (2016) 1874–1887. [PubMed: 26901771]

[56]. Adkins J, Boehle K, Henry C, Electrochemical paper-based microfluidic devices, Electrophoresis, 36 (2015) 1811–1824. [PubMed: 25820492]

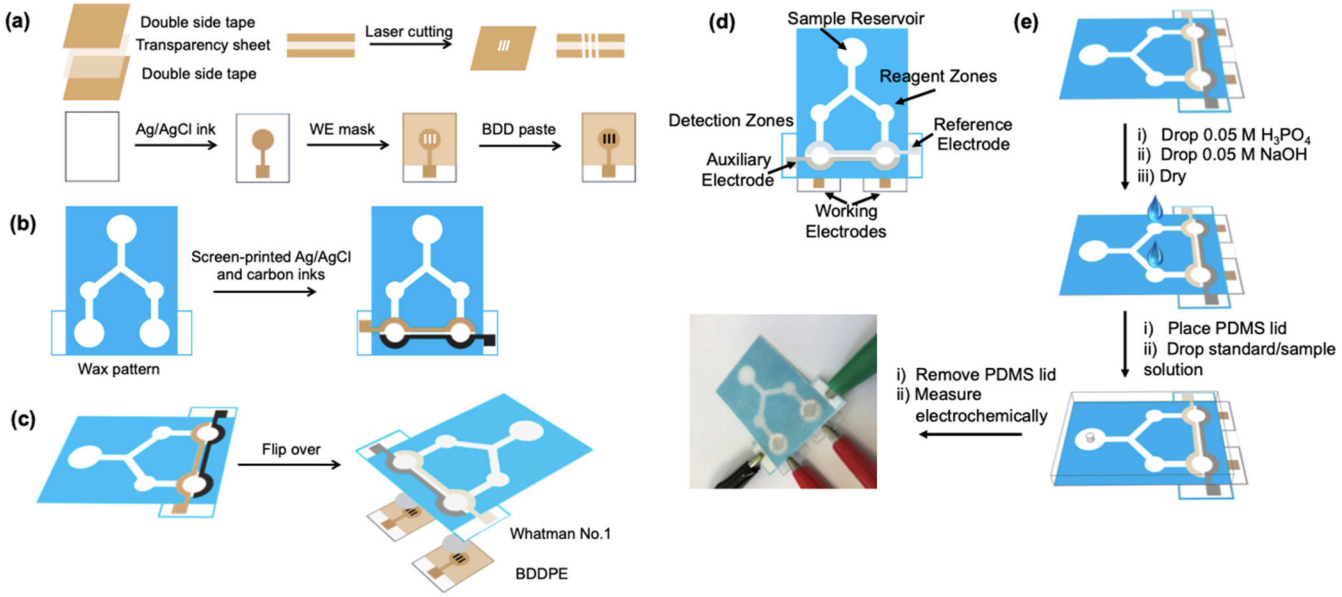

Figure 1.

Schematic for (a) fabrication of the BDDPE WE (b) fabrication of the CE and RE on wax-patterned paper (c) attachment of BDDPE WEs to paper device to fabricate Janus-ePAD (d) Janus-ePAD design and (e) operation for multiplexed detection with in situ pH adjustment.

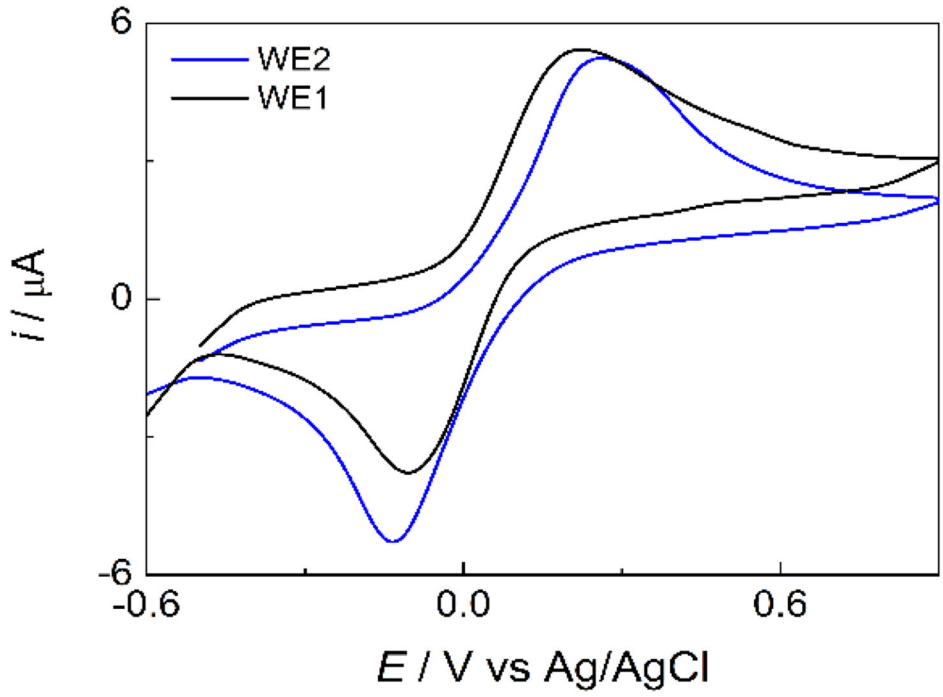

Figure 2.

Cyclic voltammograms of 4 mM $Fe(CN)_6^{4-}$ in 0.1 M KCl at BDDPE1 (black line) and BDDPE2 (blue line) on Janus-ePAD. Scan rate: 50 mV s^{-1}, WE: BDDPE.

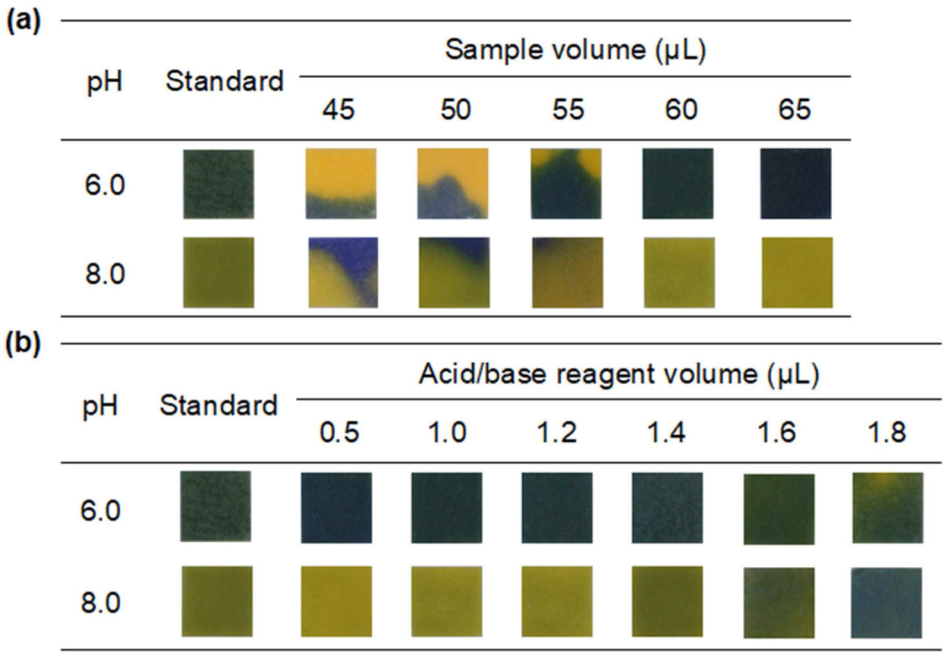

Figure 3.

Effect of parameters for in situ pH adjustment of 0.10 M PB from pH 7.0 to pH 6.0 and pH 8.0. (a) Effect of sample/reagent volume and (b) volume of H_3PO_4 and NaOH solutions on the color change of pH-indicator strip

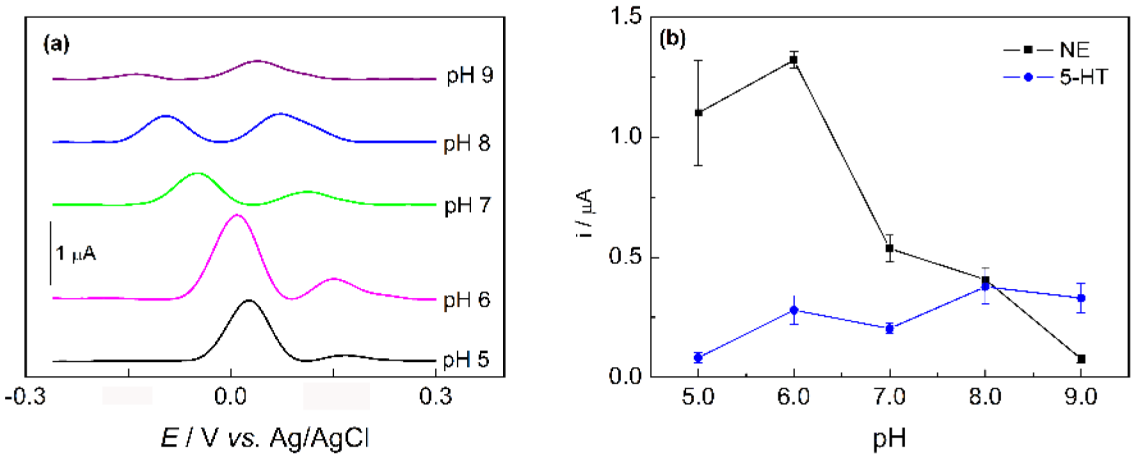

Figure 4.

(a) DPVs of 25 μM NE and 10 μM 5-HT in 0.1 M PB in the pH range of 5.0 – 9.0 at ERGO-BDDPE, note DPVs are offset for clarity. (b) The relationship of oxidation current of NE and 5-HT against pH (n = 3). DPV measurements were performed at an amplitude of 60 mV, potential increment of 4 Hz, and a pulse width of 0.05 s.

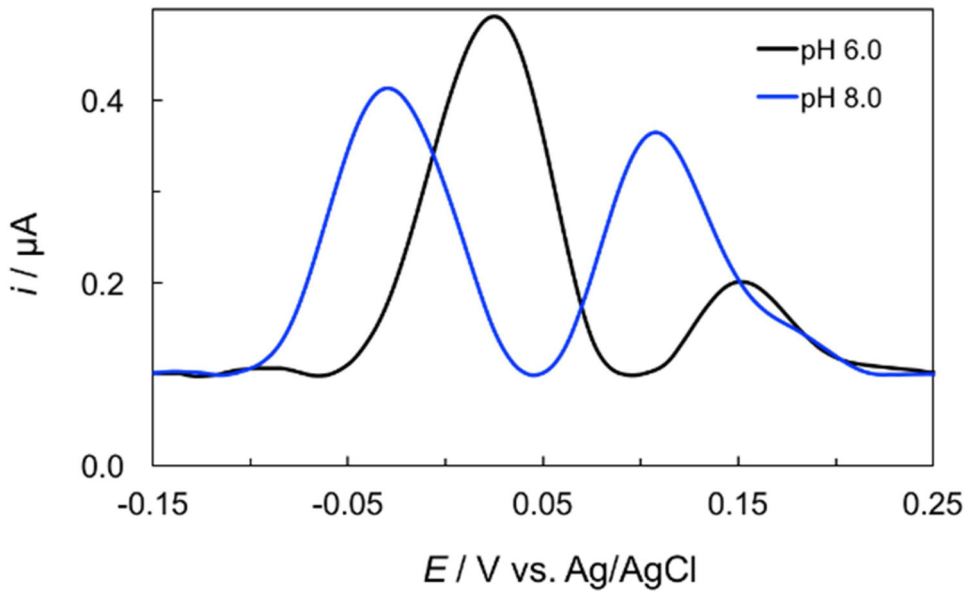

Figure 5.

DPVs of 25.0 μM NE and 10.0 μM 5-HT in 0.1 M PB on Janus-ePAD at WE1 and WE2 where pH of 0.1 M PBS was simultaneously in situ adjusted from pH 7.0 to pH 6.0 (WE1) and 8.0 (WE2), respectively. DPV measurements were performed at an amplitude of 60 mV, potential increment of 4 Hz, and a pulse width of 0.05 s.

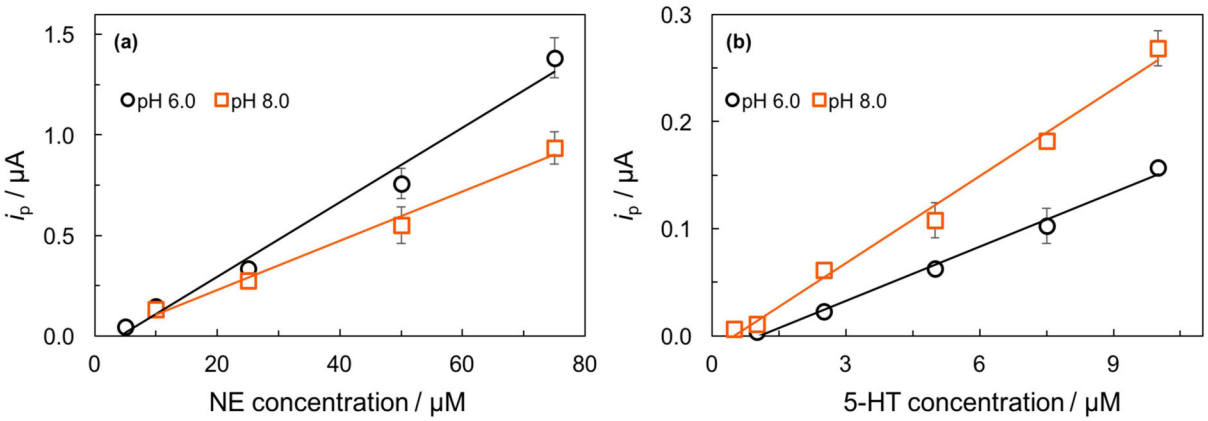

Figure 6.

Calibration curves for increasing concentration of (a) NE in the range of 5.0 – 75 μM (pH 6.0) and 10 – 75 μM (pH 8.0) and (b) 5-HT in the range of 1.0 – 10 μM (pH 6.0) and 0.5 – 10.0 μM (pH 8.0) (n=3).

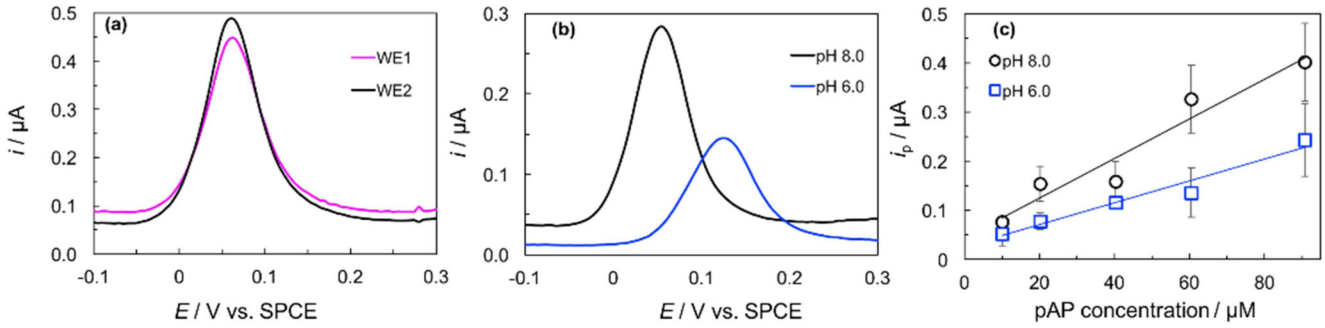

Figure 7.

(a) DPVs obtained simultaneously in the Janus-ePAD for the oxidation of 60.5 µM pAP (pH 7.0), (b) DPVs obtained for pAP under pH conditions generated in situ, (c) pAP calibration curves at pH 8.0 and pH 6.0.